Interaction of waves with frictional interfaces using summation-by-parts difference operators, 1. Weak enforcement of nonlinear boundary conditions

Jeremy E. Kozdon[*,a], Eric M. Dunham[a], Jan Nordström[b,c]

[a] *Department of Geophysics, Stanford University, 397 Panama Mall, Stanford, CA 94305, USA*

[b] *Department of Information Technology, Uppsala University, Box 337, SE-75105 Uppsala, Sweden*

[c] *Department of Aeronautics and Systems Integration, FOI, The Swedish Defence Research Agency, SE-164 90 Stockholm, Sweden*

Abstract

In this work we develop a high-order method for problems in elastodynamics with nonlinear boundary conditions. For simplicity, only 1-D problems are considered and the material is scalar elastic (deformation in only one direction). The boundary conditions considered are of a form closely related to those seen in earthquake rupture modeling and other frictional sliding problems. By using summation-by-parts finite difference operators and weak enforcement of boundary conditions with the simultaneous approximation term method, a strictly stable method is developed that dissipates energy at a slightly faster rate than the continuous solution (with the difference in energy dissipation rates vanishing as the mesh is refined). Furthermore, it is shown that unless boundary conditions are formulated in terms of characteristic variables, as opposed to the physical variables in terms of which boundary conditions are more naturally stated, the semi-discretized system of equations can become extremely stiff, preventing efficient solution using explicit time integrators.

These theoretical results are confirmed by several numerical tests demonstrating the high-order convergence rate of the method and the benefits of using strictly stable numerical methods for long time integration.

[*] Corresponding Author

Email address: jkozdon@stanford.edu (Jeremy E. Kozdon)

1. Introduction

Problems involving frictional contacts between solids are important in many fields including earthquake dynamics, fracture mechanics, and structural engineering and design. For many of these problems the material can be modeled as linear elastic with frictional sliding occurring on infinitesimally thin internal interfaces, or faults, governed by nonlinear friction laws. As relative motion occurs across the interface (with the discontinuity in displacement referred to as slip) nonlinear relations relate the slip velocity to the tractions acting on the fault.

In order to match the frictional behavior seen in experiments, the friction laws used in practice must depend not only on slip velocity and tractions acting on the fault but also, for example, on the history of sliding, frictional heat generation, and other process occurring within the fault zone. Friction laws with this more complex structure, referred to as rate-and-state friction laws, will be addressed in more detail in the companion paper [Interaction of waves with frictional interfaces using summation-by-parts difference operators, 2. Extension to full elastodynamics; Jeremy E. Kozdon, Eric M. Dunham, and Jan Nordström, submitted to J. Comp. Phys.], hereafter referred to as Part 2.

In this work we assume that the fault shear strength τ (resistance to slip) depends only on the slip velocity V through the friction law $\tau = F(V)$. Furthermore, we restrict our attention to 1-D problems and assume that the material deforms in only one direction, such that the governing equations of linear elasticity simplify to a pair of partial differential equations for one component of velocity and one component of stress (i.e., scalar elasticity). We also consider a simplified geometry containing a single fault at the boundary between a rigid substrate and the elastic material, (i.e., a one-sided fault); see Sec. 2. Most of the important properties of the scheme are more readily understood with these simplifying assumptions. In Part 2 we generalize this analysis to full elastodynamics (involving multidirectional deformation carried by a dilatational and two shear waves with orthogonal polarizations) and faults that separate two elastic bodies with differing material properties. That work also considers the more general class of rate-and-state friction laws.

In this work, we use summation-by-parts (SBP) finite difference methods [Kreiss and Scherer, 1974, 1977, Strand, 1994, Carpenter et al., 1999, Mattsson and Nordström, 2004]. The advantage of these methods is that after appropriate boundary treatment the numerical methods can be proven to mimic the energy dissipation properties of the continuous problem, leading

to what is known as strict stability [Gustafsson et al., 1996] (see Sec. 3).

A field, $v(y)$, is discretized on a uniform grid spanning the unit interval:

$$v_i = v(y_i),\ y_i = i\ h,\ i = 0, \ldots, N, \tag{1}$$

where $h = 1/N$ is the grid spacing and y_0 and y_N are on the left and right boundaries, respectively. A difference approximation to the first derivative is said to be of SBP form if it can be written as

$$\frac{\partial v}{\partial y} \approx \boldsymbol{H}^{-1}\boldsymbol{Q}\ \boldsymbol{v}, \tag{2}$$

where $\boldsymbol{H}$ is a symmetric positive definite matrix, $\boldsymbol{Q}$ is an almost skew-symmetric matrix with $\boldsymbol{Q}^T + \boldsymbol{Q} = \mathbf{diag}(-1, 0, \ldots, 0, 1)$, and the vector $\boldsymbol{v} = (v_0, v_1, \ldots, v_N)^T$ is the grid data. For instance, the second order SBP operator is [Kreiss and Scherer, 1974]

$$\boldsymbol{H} = h\ \mathbf{diag}\left[\tfrac{1}{2}\quad 1\quad 1\quad \cdots\quad 1\quad \tfrac{1}{2}\right],\ \boldsymbol{Q} = \frac{1}{2}\begin{bmatrix} -1 & 1 & & & \\ -1 & 0 & 1 & & \\ & \ddots & \ddots & \ddots & \\ & & -1 & 0 & 1 \\ & & & -1 & 1 \end{bmatrix}. \tag{3}$$

Defining the continuous and discrete inner products,

$$(u, v) = \int_0^1 u(y)\ v(y)\ dy \quad \text{and} \quad (\boldsymbol{u}, \boldsymbol{v})_h = \boldsymbol{u}^T\ \boldsymbol{H}\boldsymbol{v}, \tag{4}$$

it becomes clear why these methods are called SBP methods as they mimic the integration-by-parts property of the continuous problem,

$$\left(v, \frac{dv}{dy}\right) = \int_0^1 v\ \frac{dv}{dy}\ dy = \frac{1}{2}\left[v(1)^2 - v(0)^2\right], \tag{5}$$

$$(\boldsymbol{v}, \boldsymbol{H}^{-1}\boldsymbol{Q}\boldsymbol{v})_h = \boldsymbol{v}^T\ \boldsymbol{Q}\ \boldsymbol{v} = \frac{1}{2}\boldsymbol{v}^T\ (\boldsymbol{Q} + \boldsymbol{Q}^T)\ \boldsymbol{v} = \frac{1}{2}(v_N^2 - v_0^2). \tag{6}$$

SBP operators are constructed from central difference methods, with orders $q = 2, 4, 6, 8, \ldots$ in the interior, and transition near boundaries to one-sided difference methods in a manner that maintains the SBP property. Generally, the transition to one-sided near the boundary lowers the local accuracy of the method to r; hence, the global accuracy of the method is $p = r+1$ [Gustafsson, 1975, Svärd and Nordström, 2007]. There are two classes of

SBP operators: diagonal norm (diagonal $\boldsymbol{H}$) and block norm operators (non-diagonal $\boldsymbol{H}$). The diagonal norm operators have interior accuracy $q = 2s$ ($s = 1, 2, \dots$) and boundary accuracy $r = s$, so the global accuracy is $p = s+1$, whereas block norm operators can have boundary accuracy $r = 2s-1$ and thus global accuracy $p = 2s$. There are drawbacks to using the block norm operators, the most prominent being difficulties in proving stability for problems which involve variable coefficients and/or coordinate transforms [Nordström and Carpenter, 2001, Olsson, 1995, Nordström, 2006]. In this work we exclusively consider the diagonal norm operators and methods are referred to by their global accuracy.

Using SBP methods, along with suitable boundary treatment, it is possible to design difference schemes that mimic the energy dissipation properties of the continuous partial differential equation (PDE), resulting in a provably stable discretization. There are numerous methods for incorporating boundary conditions; the two considered in this work are the *injection* method, which enforces boundary conditions strongly, and the *simultaneous approximation term* (SAT) method [Carpenter et al., 1994], which enforces boundary conditions weakly. In the injection method the grid values at the boundary points are modified so that they strictly satisfy the boundary conditions. Though this is conceptually straightforward, the method destroys the SBP property of the operator and stability can be difficult or impossible to prove [Gustafsson et al., 1996]. With SAT these grid values are not directly modified, but a penalty term is added to the semi-discrete equations so that the difference operator is penalized for not satisfying the boundary conditions. With a carefully chosen penalty parameter, stability and accuracy are guaranteed.

The remainder of this paper is as follows: In Sec. 2 well-posedness and the energy dissipation rate for the continuous problem are established. The discrete method is then discussed in Sec. 3 along with three procedures for including boundary conditions: the injection method and two formulations of the SAT method. The SAT method leads to numerical methods which dissipate energy at least as fast as the continuous solution (and the difference in the rates goes to zero as the mesh is refined) thus ensuring strict stability. The computational benefits and drawbacks of the two SAT methods are discussed in Sec. 3.4 and in Sec. 4 computational results demonstrate the theoretical results. Conclusions are presented in Sec. 5.

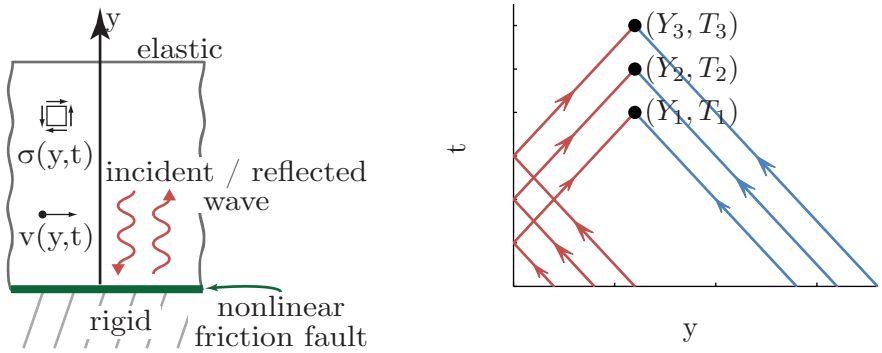

(a) Problem configuration (b) Method of characteristics

Figure 1: Assuming that the initial conditions are such that there is no right propagating wave, the solution at a point (Y,T) is a combination of an incident wave (from the initial condition) and a wave reflected from the fault.

2. Continuous Problem: Well-Posedness and Energy Dissipation

Consider a 1-D elastic medium in contact with a rigid substrate along a frictional interface (or fault) located at $y = 0$ (Figure 1a). The governing equations in the elastic medium are momentum conservation and the time derivative of Hooke's law,

$$\rho \frac{\partial v}{\partial t} = \frac{\partial \sigma}{\partial y} \quad \text{and} \quad \frac{\partial \sigma}{\partial t} = G \frac{\partial v}{\partial y}, \tag{7}$$

where v is the particle velocity tangential to the fault, σ is the component of stress that exerts a shear traction on the fault in the direction of the particle velocity, ρ is density, and G is shear modulus. The material properties are taken to be spatially uniform in this work. These equations can be written as a first order hyperbolic system that can be symmetrized by introducing the vector $\boldsymbol{q} = [\sqrt{\rho/2}\, v \quad \sigma/\sqrt{2G}]^T$:

$$\frac{\partial \boldsymbol{q}}{\partial t} = \begin{bmatrix} 0 & c_s \\ c_s & 0 \end{bmatrix} \frac{\partial \boldsymbol{q}}{\partial y} = \boldsymbol{A} \frac{\partial \boldsymbol{q}}{\partial y}, \tag{8}$$

where $c_s = \sqrt{G/\rho}$ is the shear wave speed.

To fully specify the problem, boundary conditions are needed; for now we assume a semi-infinite medium so the only boundary is at the fault. In order

to determine the number of boundary conditions required, the diagonalized form of the governing equations is considered. This is

$$\frac{\partial \boldsymbol{w}}{\partial t} = \begin{bmatrix} -c_s & 0 \\ 0 & c_s \end{bmatrix} \frac{\partial \boldsymbol{w}}{\partial y}, \quad \boldsymbol{w} = \begin{bmatrix} \sigma - Z\ v \\ \sigma + Z\ v \end{bmatrix} = \begin{bmatrix} w^+ \\ w^- \end{bmatrix}, \tag{9}$$

where w^+ and w^- are the characteristic variables associated with shear waves propagating with speeds $+c_s$ and $-c_s$, respectively, and $Z = \rho\ c_s = G/c_s$ is the shear impedance. In this form it is clear that one boundary condition is required at $y = 0$ relating the wave going into the fault, $w^-(0,t)$, to the wave coming out of the fault, $w^+(0,t)$ [Kreiss, 1970]:

$$w^+(0,t) = \mathcal{W}^+\left(w^-(0,t)\right) \tag{10}$$

(specific forms of $\mathcal{W}^+(w^-)$ will be discussed shortly).

Letting the initial condition be

$$w^{\pm}(y,0) = \tilde{w}^{\pm}(y),\ \tilde{w}^{\pm}(y) = 0 \text{ if } y < 0, \tag{11}$$

a solution can be found using the method of characteristics (see Figure 1b):

$$w^+(y,t) = \mathcal{W}^+\left(\tilde{w}^-(c_s\ t - y)\right) + \tilde{w}^+(c_s\ t - y), \tag{12}$$

$$w^-(y,t) = \tilde{w}^-(c_s\ t + y). \tag{13}$$

For the problem to be well-posed a solution must exist, be unique, and satisfy the energy estimate [Gustafsson et al., 1996] (the energy estimates must depend continuously on the initial condition)

$$\|\boldsymbol{q}(\cdot,t)\| \leq K_c e^{\alpha_c t} \|\boldsymbol{q}(\cdot,0)\|. \tag{14}$$

In (14) K_c and α_c are constants independent of the solution. In this work, the norm is taken to be the physical energy in the solution,

$$\begin{aligned} \|\boldsymbol{q}(\cdot,t)\|^2 =& \int_0^\infty \boldsymbol{q}(y,t)\boldsymbol{q}(y,t)^T\ dy \\ =& \frac{\rho}{2}\int_0^\infty v(y,t)^2\ dy + \frac{1}{2G}\int_0^\infty \sigma(y,t)^2\ dy, \end{aligned} \tag{15}$$

where the first term is the kinetic energy and the second the elastic strain energy. If it can be shown that the solution dissipates energy,

$$\frac{d\|q\|^2}{dt} \leq 0, \tag{16}$$

then by integration (14) holds with $\alpha_c = 0$ and $K_c = 1$. For the problem (8) we have

$$\begin{aligned}\frac{d}{dt}\|\boldsymbol{q}(\cdot,t)\|^2 &= \int_0^\infty \boldsymbol{q}(y,t)^T \, \frac{\partial \boldsymbol{q}}{\partial t}(y,t) \, dy \\ &= \int_0^\infty \boldsymbol{q}(y,t)^T A \, \frac{\partial \boldsymbol{q}}{\partial y}(y,t) \, dy \\ &= \left[v\,(y,t) \;\; \sigma\,(y,t)\right]_{y=0}^{\infty} \\ &= -\, v\,(0,t) \;\; \sigma\,(0,t)\,, \end{aligned} \tag{17}$$

where (17) follows from integration by parts and the assumption that the fields go to zero as $y \to \infty$; it is possible to generalize this result to a prestressed material with background (nonzero) values of particle velocity and stress on top of which time-dependent perturbations propagate. The term $\sigma \; v$ is the energy flux across the boundary, a well-known result from continuum mechanics [Malvern, 1977]. In order to show that (17) is non-positive, specific boundary formulations must be considered.

Remark: For linear problems with linear boundary conditions energy dissipation implies uniqueness and thus well-posedness (assuming existence). For problems with nonlinear boundary conditions energy dissipation only does not imply uniqueness (as will be shown below).

Remark: If a problem is well-posed with a specific boundary condition $w^+(0,t) = \mathcal{W}^+\left(w^-(0,t)\right)$, then the problem remains well-posed if the boundary condition is modified to include a time-dependent forcing function $g(t)$ as $w^+(0,t) = \mathcal{W}^+(w^-(0,t)) + g(t)$ [Gustafsson et al., 1996]. Note in this case the solution energy $\|\boldsymbol{q}\|^2$ is permitted to grow in a controlled manner in time due to the forcing function.

2.1. Linear Boundary Conditions

The simplest form for $\mathcal{W}^+\left(w^-\right)$ is a linear function,

$$\mathcal{W}^+(w^-) = R\, w^-, \tag{18}$$

where the constant R is a reflection coefficient. The energy dissipation rate (17) with this linear boundary condition is

$$\begin{aligned}\frac{d}{dt}\|\boldsymbol{q}(\cdot,t)\|^2 &= -\,\frac{1}{4Z}\left[w^-(0,t) + w^+(0,t)\right]\left[w^-(0,t) - w^+(0,t)\right] \\ &= -\,\frac{1}{4Z}\left(1 - R^2\right) w^-(0,t)^2, \end{aligned} \tag{19}$$

where the physical variables have been written in terms of the characteristic variables using (9). For $-1 \leq R \leq 1$ there is no growth in energy, Since this is a linear boundary condition, these is a unique solution, and since the solution exists, the problem is well-posed.

It is more common for boundary conditions in elastodynamics to be formulated in terms of the physical variables (velocity and stress). We consider boundary conditions that express the frictional resistance to slip across the fault as a function of the slip velocity. Specifically, we define the slip velocity $V(t)$ as the discontinuity in particle velocity across the fault and the fault shear strength $\tau(t)$ as the fault's frictional resistance to sliding, which is equal to the shear traction acting on the fault; for a one-sided fault these are

$$V(t) \equiv v(0,t) \text{ and } \tau(t) \equiv \sigma(0,t). \tag{20}$$

The simplest relation between τ and V is a linear friction law,

$$\tau = \alpha V, \tag{21}$$

where α is a constant. Physically, this friction law corresponds to a thin layer of Newtonian fluid between the elastic solid and the rigid substrate (α is the product of the fluid viscosity and the layer thickness).

The boundary condition in terms of the characteristic variables (18) and the boundary condition in terms of the physical variables (21) are equivalent, with

$$R = \frac{\alpha/Z - 1}{\alpha/Z + 1}, \tag{22}$$

and $-1 \leq R \leq 1$ if $\alpha \geq 0$ ($Z > 0$ by definition). With the boundary condition formulated in terms of the physical variables, the energy dissipation rate (17) is

$$\frac{d}{dt}\|\boldsymbol{q}(\cdot,t)\|^2 = -\,\alpha\, v\,(0,t)^2\,, \tag{23}$$

and the linear friction law (21) leads to a well-posed problem if $\alpha \geq 0$.

2.2. Nonlinear Boundary Conditions

As mentioned in the introduction, nonlinear friction laws,

$$\tau = F(V), \tag{24}$$

are necessary to account for the behavior seen in laboratory experiments. An example of a friction law closely related to those used in earthquake rupture models is

$$F(V) = \beta \operatorname{arcsinh}(\gamma V), \tag{25}$$

where β and γ are positive constants. Rate-and-state friction laws have the form of (25) except with γ evolving in time according to a differential evolution equation. With the nonlinear boundary condition (24), the energy dissipation rate is

$$\frac{d}{dt}\|\boldsymbol{q}(\cdot,t)\|^2 = -V(t)\,\tau(t) = -V(t)F(V(t)), \tag{26}$$

and the solution dissipates energy if the nonlinear friction law takes the sign of its argument (or zero), that is, $\operatorname{sign}(F(V)) = \operatorname{sign}(V)$ or 0. Physically, the quantity $V\,\tau$ is the rate at which mechanical energy is converted to heat during frictional sliding of the fault.

For the problem to be well-posed a solution must exist and be unique for all initial data $\boldsymbol{q}(y,0)$; these two points will be addressed with the method of characteristics and the energy method, respectively, below.

Existence via the method of characteristics

In order to show existence of a solution we derive conditions on $F(V)$ such that the boundary condition is (implicitly) expressible in the form $w^+(0,t) = \mathcal{W}^+(w^-(0,t))$, where $\mathcal{W}^+(w^-)$ is unique (i.e., single valued). Existence then follows by the method of characteristics; see Figure 1b and (12)-(13).

The restrictions that are imposed on $F(V)$ can be understood graphically. To do this, first note that τ and V can be written as

$$V(t) = v(0,t) = \frac{1}{2Z}\left[w^-(0,t) - \mathcal{W}^+\left(w^-(0,t)\right)\right], \tag{27}$$

$$\tau(t) = \sigma(0,t) = \frac{1}{2}\left[w^-(0,t) + \mathcal{W}^+\left(w^-(0,t)\right)\right]. \tag{28}$$

Hence, a unique function $\mathcal{W}^+(w^-)$ exists for a friction law $F(V)$ only if for every w^- there is a unique V that satisfies

$$\tau = w^- - Z\,V = F(V), \tag{29}$$

where the first equality is due to (27) and (28) and the second is due to (24). The relationship $\tau = w^- - ZV$ is known as the radiation damping response

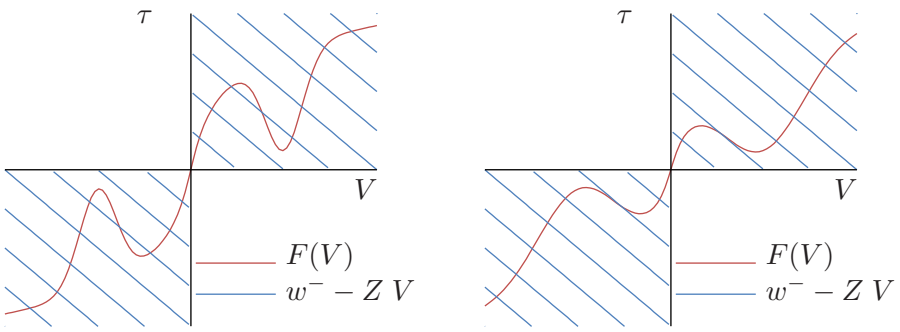

(a) Invalid friction law

(b) Valid friction law

Figure 2: Plot of two friction laws $\tau = F(V)$ and radiation damping lines $\tau = w^- - Z\ V$ for various w^- values. Multiple crossings of a radiation damping line and the friction law indicate that the friction law is invalid. The curves are only shown in the valid velocity regions, i.e. where $F(V)\ V \geq 0$.

[Rice, 1993], and arises frequently in many boundary integral equation formulations of elastodynamics [Cochard and Madariaga, 1994, Geubelle and Rice, 1995]. Figure 2 shows both of these expressions for τ versus V for two different nonlinear friction laws. For the friction law in Figure 2a some values of w^- give rise to multiple V which satisfy (29), in which case there is not a unique $\mathcal{W}^+(w^-)$. The friction law in Figure 2b has a unique V which satisfies (29) for every w^-.

This condition can be expressed by rewriting (24) using the characteristic variables:

$$\frac{1}{2}\left[w^- + \mathcal{W}^+(w^-)\right] = F\left(\frac{1}{2Z}\left[w^- - \mathcal{W}^+(w^-)\right]\right). \tag{30}$$

Then by the implicit function theorem there is a unique $\mathcal{W}^+(w^-)$ if

$$\begin{aligned} 0 \neq & \frac{d}{d\,\mathcal{W}^+}\left[\frac{1}{2}\left(w^- + \mathcal{W}^+\right) - F\left(\frac{1}{2Z}\left(w^- - \mathcal{W}^+\right)\right)\right] \\ = & \frac{1}{2} + \frac{1}{2Z}F'\left(\frac{1}{2Z}\left(w^- - \mathcal{W}^+\right)\right). \end{aligned} \tag{31}$$

This imposes the restriction $F'(V) \neq -Z$ for $V \in \mathbb{R}$ in order for a solution to exist.

Algorithm 1 Calculate V using bracketed Newton's method

Require: Initial value V
  Initialize: $V_{\min} \leftarrow \min(0, w^-/Z)$, $V_{\max} \leftarrow \max(0, w^-/Z)$
  if $V > V_{\max}$ or $V < V_{\min}$ **then**
    $V \leftarrow (V_{\max} + V_{\min})/2$
  end if
  while not converged **do**
    $g \leftarrow F(V) + Z\,V - w^-$
    $dg \leftarrow F'(V) + Z$
    if $g < 0$ **then**
      $V_{\min} \leftarrow V$
    else
      $V_{\max} \leftarrow V$
    end if
    $V \leftarrow V - g/dg$
    if $V > V_{\max}$ or $V < V_{\min}$ **then**
      $V \leftarrow (V_{\max} + V_{\min})/2$
    end if
  end while

Remark: Given a value for w^-, the corresponding $\mathcal{W}^+(w^-)$ can be found using a bracketed Newton's method to solve for V in (29), using the bracket $V \in [\min(0, w^-/2), \max(0, w^-/2)]$ (see Figure 2b), and $\mathcal{W}^+$ can be calculated using (27). This procedure is outlined in Algorithm 1 where $g(V) = F(V) + Z\,V - w^-$.

Uniqueness via the energy method

Assume that $\boldsymbol{q}_1$ and $\boldsymbol{q}_2$ are solutions to (8) with boundary condition (24), and that $\boldsymbol{q}_1(y, 0) = \boldsymbol{q}_2(y, 0)$; then $\boldsymbol{\Delta} = \boldsymbol{q}_1 - \boldsymbol{q}_2$ satisfies

$$\frac{\partial \boldsymbol{\Delta}}{\partial t} = \boldsymbol{A}\frac{\partial \boldsymbol{\Delta}}{\partial y}, \quad \boldsymbol{\Delta}(y, 0) = \boldsymbol{0}, \tag{32}$$

$$\tau_1 - \tau_2 = F(V_1) - F(V_2). \tag{33}$$

The energy dissipation rate of this problem is then

$$\frac{d\|\boldsymbol{\Delta}(\cdot, t)\|^2}{dt} = -\left[F(V_1) - F(V_2)\right](V_1 - V_2) = -F'(V)\,(V_1 - V_2)^2\,, \tag{34}$$

where the last equality is due to the intermediate value theorem for some $V \in [V_1, V_2]$. Thus if $F'(V) \geq 0$ for all V, then $d\|\boldsymbol{\Delta}(\cdot, t)\|^2/dt \leq 0$ for all t.

Hence, since initially $\|\boldsymbol{\Delta}(\cdot,0)\|^2 = 0$ we have that $\|\boldsymbol{\Delta}(\cdot,t)\|^2 = 0$ (implying $\boldsymbol{\Delta}(y,t) = 0$) for all t and the solution is unique ($\boldsymbol{q}_1 = \boldsymbol{q}_2$).

The problem is well-posed (14) if the nonlinear friction law satisfies

$$V\ F(V) \geq 0, \tag{35}$$

$$F'(V) > 0 \text{ for all } V \in \mathbb{R}, \tag{36}$$

where (35) guarantees energy dissipation and (36) uniqueness of the solution.

Remark: All friction laws used in practice satisfy the conditions $F(V)V \geq 0$ and $F'(V) \geq 0$. In the appendix we prove, using a different energy norm, that the problem is well-posed for all $F(V)$ which satisfy $F'(V) \neq -Z$ (the restriction imposed by the implicit function theorem (31)). This means that (35) and (36) can be seen as physical requirements that lead to well-posedness, whereas the general mathematical requirement is $F'(V) \neq -Z$; see the appendix for more details.

The nonlinear reflection coefficient $R(w^-)$ implied by a nonlinear friction law $F(V)$ satisfies $-1 \leq R(w^-) \leq 1$. Namely, recalling that $V = [w^- - \mathcal{W}^+(w^-)]/(2Z)$, we can rewrite (30) as

$$\frac{1}{2}\left[w^- + \mathcal{W}^+(w^-)\right] = \alpha(w^-)\ \frac{1}{2Z}\left[w^- - \mathcal{W}^+(w^-)\right], \tag{37}$$

$$\alpha(w^-) = \lim_{w \to w^-} \frac{F\left([w - \mathcal{W}^+(w)]/(2Z)\right)}{[w - \mathcal{W}^+(w)]/(2Z)}, \tag{38}$$

where $\alpha(w^-) \geq 0$ since $\text{sign}(F(V)) = \text{sign}(V)$ or 0 (if $F(V) = \alpha\ V$ then $\alpha(w^-) = \alpha$). Solving for $\mathcal{W}^+(w^-)$ gives

$$W^+(w^-) = \left[\frac{\alpha(w^-)/Z - 1}{\alpha(w^-)/Z + 1}\right] w^- = R(w^-)\ w^-, \tag{39}$$

which satisfies $-1 \leq R(w^-) \leq 1$.

If the boundary condition is specified in terms of the characteristic variables, the energy dissipation rate (17) becomes

$$\frac{d}{dt}\|\boldsymbol{q}(\cdot,t)\|^2 = -\frac{1}{4Z}\left[1 - R(w^-(0,t))^2\right] w^-(0,t)^2, \tag{40}$$

where the nonlinear reflection coefficient is defined in (39); the problem is well-posed if $-1 \leq R(w^-) \leq 1$ for all $w^- \in \mathbb{R}$, as is the case if (36) is satisfied.

3. Discrete Formulation: Stability and Energy Dissipation

As noted above, stable and accurate finite difference methods can be developed using SBP operators. A method of lines discretization of the governing equation (8) is

$$\frac{d\boldsymbol{q}}{dt} = \left(\boldsymbol{H}^{-1}\boldsymbol{Q} \otimes \boldsymbol{A}\right) \boldsymbol{q}, \tag{41}$$

$$\boldsymbol{q} = \begin{bmatrix} \boldsymbol{q}_0^T & \boldsymbol{q}_1^T & \cdots & \boldsymbol{q}_N^T \end{bmatrix}^T, \ \boldsymbol{q}_i = \begin{bmatrix} \sqrt{\frac{\rho}{2}}\, v_i & \frac{1}{\sqrt{2G}}\, \sigma_i \end{bmatrix}^T, \tag{42}$$

where v_i and σ_i are collocated (i.e., an unstaggered grid is used) and $\otimes$ is the Kronecker product of two matrices defined by

$$\boldsymbol{A} \otimes \boldsymbol{B} = \begin{bmatrix} A_{00}\boldsymbol{B} & A_{01}\boldsymbol{B} & \dots & A_{0N}\boldsymbol{B} \\ A_{10}\boldsymbol{B} & A_{11}\boldsymbol{B} & & \\ \vdots & & \ddots & \\ A_{M0}\boldsymbol{B} & & & A_{MN}\boldsymbol{B} \end{bmatrix}, \tag{43}$$

where $\boldsymbol{A}$ is $(M+1)\times(N+1)$. Two Kronecker product identities are needed for the analysis that follows:

$$(\boldsymbol{A} \otimes \boldsymbol{B})^T = \boldsymbol{A}^T \otimes \boldsymbol{B}^T, \tag{44}$$

$$(\boldsymbol{A} \otimes \boldsymbol{B})(\boldsymbol{C} \otimes \boldsymbol{D}) = (\boldsymbol{A}\boldsymbol{C}) \otimes (\boldsymbol{B}\boldsymbol{D}). \tag{45}$$

The discrete energy norm can be defined in a manner analogous to the continuous energy norm (15) as

$$\|\boldsymbol{q}\|_h^2 = \boldsymbol{q}^T \left(\boldsymbol{H} \otimes \boldsymbol{I}_2\right) \boldsymbol{q} = \frac{\rho}{2}\boldsymbol{v}^T \boldsymbol{H} \boldsymbol{v} + \frac{1}{2G}\boldsymbol{\sigma}^T \boldsymbol{H} \boldsymbol{\sigma}, \tag{46}$$

where the first term is the kinetic energy, the second the elastic strain energy, and $\boldsymbol{I}_2 = \mathbf{diag}(1,1)$. The difference operator is said to be strictly stable [Gustafsson et al., 1996] if

$$\|\boldsymbol{q}(t)\|_h^2 \leq K_d e^{\alpha_d t} \|\boldsymbol{q}(0)\|_h^2, \quad \alpha_d \leq \alpha_c + \mathcal{O}(h), \tag{47}$$

where α_d and K_d are constants independent of the initial conditions and α_c is the growth rate for the continuous problem in (14). If it can be shown that the discrete solution dissipates energy at least as fast as the continuous solution, and that the energy dissipation rate converges to the true rate under refinement, then (47) follows.

For the discrete method to be fully specified, the boundary conditions must be included. In this work two methods are considered: the injection method (strong enforcement) and the SAT method (weak enforcement). For simplicity, the right boundary is initially ignored in the presentation of the boundary treatment.

3.1. SBP + Injection Method

In the injection method, boundary conditions are enforced *strongly* so that the boundary values, $\boldsymbol{q}_0 = [\sqrt{\rho/2}\ v_0 \quad \sigma_0/\sqrt{2G}]^T$, strictly satisfy the boundary conditions. This can be done by modifying only the characteristic variable associated with waves propagating from the boundary into the medium [Kreiss, 1970, Thompson, 1987, 1990, Oliger and Sundstrom, 1978]; we assume that the boundary condition is in characteristic form (10). In order to understand how the injection method works, consider a single forward Euler step with the injection method. First, the discretized PDE (41) is used to update the solution from $\boldsymbol{q}^n \equiv \boldsymbol{q}(t^n)$ to $\boldsymbol{q}^{n+1} \equiv \boldsymbol{q}(t^{n+1})$, where $t^{n+1} = t^n + \Delta t$, and then the boundary values are overwritten so that they satisfy the boundary condition. Algorithmically this is

$$\boldsymbol{q}^{n+1} \leftarrow \boldsymbol{q}^n + \Delta t\ \left(\boldsymbol{H}^{-1}\boldsymbol{Q} \otimes \boldsymbol{A}\right) \boldsymbol{q}^n, \tag{48}$$

$$\boldsymbol{q}_0^{n+1} \leftarrow \frac{1}{2\sqrt{2G}} \begin{bmatrix} (w_0^-)^{n+1} - \mathcal{W}^+((w_0^-)^{n+1}) \\ (w_0^-)^{n+1} + \mathcal{W}^+((w_0^-)^{n+1}) \end{bmatrix}, \tag{49}$$

where $(w_0^\pm)^{n+1} = \sigma_0^{n+1} \mp Z\ v_0^{n+1}$ and $\leftarrow$ denotes assignment. It is easy to verify that in going from (48) to (49) only w_0^+ (the characteristic variable propagating out of the fault) is modified and w_0^- (the characteristic variable propagating into the fault) remains unchanged.

This procedure can be generalized to the system of ordinary differential equations (ODEs):

$$\frac{d\boldsymbol{q}}{dt} = \left(\boldsymbol{H}^{-1}\boldsymbol{Q} \otimes \boldsymbol{A}\right) \hat{\boldsymbol{q}}, \tag{50}$$

$$\hat{\boldsymbol{q}}_0 = \frac{1}{2\sqrt{2G}} \begin{bmatrix} w_0^- - \mathcal{W}^+(w_0^-) \\ w_0^- + \mathcal{W}^+(w_0^-) \end{bmatrix} \equiv \begin{bmatrix} \sqrt{\frac{\rho}{2}}\ \hat{v}_0 \\ \frac{1}{\sqrt{2G}}\ \hat{\sigma}_0 \end{bmatrix}, \tag{51}$$

$$\hat{\boldsymbol{q}}_i = \boldsymbol{q}_i, \quad i = 1, 2, \ldots, \tag{52}$$

and when the ODEs are integrated the solution $\hat{\boldsymbol{q}}$ always satisfies the boundary condition by construction.

Since the injection method amounts to modifying the difference operator, the SBP property of the operator is lost and, in general, it is not possible to prove that the resulting method satisfies the stability condition (47) [Gustafsson et al., 1996, Mattsson, 2003]. This can lead to unbounded energy growth in the numerical solution, as will be seen in the computational results below.

3.2. SBP + SAT (Simultaneous Approximation Term) method

In the SAT method, boundary conditions are *weakly* enforced through a penalty term added directly to the semi-discretized system:

$$\frac{d\boldsymbol{q}}{dt} = \left(\boldsymbol{H}^{-1}\boldsymbol{Q} \otimes \boldsymbol{A}\right)\boldsymbol{q} + \boldsymbol{H}^{-1}\boldsymbol{e}_0 \otimes \boldsymbol{\Sigma}\boldsymbol{B}\left(\boldsymbol{q}_0\right), \tag{53}$$

$$\boldsymbol{e}_0 = \begin{bmatrix}1 & 0 & \cdots & 0\end{bmatrix}^T \tag{54}$$

where $\boldsymbol{B}(\boldsymbol{q}_0)$ is a function for which $\boldsymbol{B}(\boldsymbol{q}_0) = \boldsymbol{0}$ when the boundary data $\boldsymbol{q}_0$ satisfies the friction law exactly, and the penalty matrix $\boldsymbol{\Sigma}$ will be chosen so that the method dissipates energy at least as fast as the continuous solution (with the true rate reached under grid refinement). The major advantage of weak enforcement of the boundary conditions is that the SBP property of the operator is preserved and, as we will see, this allows for the development of a numerical method that satisfies the strict stability condition (47).

Two versions of the boundary term $\boldsymbol{B}(\boldsymbol{q}_0)$ are considered in this work: the non-characteristic,

$$\boldsymbol{B}_{nc}(\boldsymbol{q}_0) = \begin{bmatrix}1\\1\end{bmatrix}[\sigma_0 - F(v_0)], \tag{55}$$

and the characteristic,

$$\boldsymbol{B}_{c}(\boldsymbol{q}_0) = \begin{bmatrix}1\\1\end{bmatrix}\left[w_0^+ - \mathcal{W}^+(w_0^-)\right], \tag{56}$$

formulations of the boundary condition. For both formulations it can be assumed without loss of generality that $\boldsymbol{\Sigma} = \mathbf{diag}(\Sigma_1, \Sigma_2)$.

The energy dissipation rate of the method is

$$\begin{aligned}\frac{d}{dt}\|\boldsymbol{q}(t)\|_h^2 =& \frac{d\boldsymbol{q}^T}{dt}\left(\boldsymbol{H} \otimes \boldsymbol{I}_2\right)\boldsymbol{q} + \boldsymbol{q}^T(\boldsymbol{H} \otimes \boldsymbol{I}_2)\frac{d\boldsymbol{q}}{dt}\\ =& \boldsymbol{q}^T\left[\left(\boldsymbol{Q}^T + \boldsymbol{Q}\right) \otimes \boldsymbol{A}\right]\boldsymbol{q} + 2\boldsymbol{q}^T\left[\boldsymbol{e}_0 \otimes \boldsymbol{\Sigma}\boldsymbol{B}(\boldsymbol{q}_0)\right]\\ =& -\boldsymbol{q}_0^T\boldsymbol{A}\boldsymbol{q}_0 + 2\boldsymbol{q}_0^T\boldsymbol{\Sigma}\boldsymbol{B}(\boldsymbol{q}_0)\\ =& -v_0\,\sigma_0 + 2\boldsymbol{q}_0^T\boldsymbol{\Sigma}\boldsymbol{B}(\boldsymbol{q}_0),\end{aligned} \tag{57}$$

where (57) follows from the SBP property; see (6). To complete the calculation and derive the penalty matrix $\boldsymbol{\Sigma}$, the two boundary formulations, (55) and (56), are considered separately.

Non-Characteristic Boundary Treatment:

The penalty matrix, $\mathbf{\Sigma}$, can be determined by substituting (55) into (57):

$$\frac{d}{dt}\|\boldsymbol{q}(t)\|_h^2 = -\, v_0\, \sigma_0 + \left(\sqrt{2\rho}\, v_0\, \Sigma_1 + \sqrt{\frac{2}{G}}\, \sigma_0\, \Sigma_2\right)\left[\sigma_0 - F(v_0)\right]. \tag{58}$$

Picking $\Sigma_1 = 1/\sqrt{2\rho}$ and $\Sigma_2 = 0$, the scheme dissipates energy at the rate

$$\frac{d}{dt}\|\boldsymbol{q}(t)\|_h^2 = -\, v_0 F(v_0) \leq 0. \tag{59}$$

Interpreting the slip velocity as $V = v_0$ and the fault strength as $\tau = F(v_0)$, rather than $\tau = \sigma_0$, the method dissipates energy at the same rate as the continuous problem (17) and is strictly stable (note there is no additional damping with this method). In summary, the non-characteristic difference method is

$$\frac{d\boldsymbol{q}}{dt} = \left(\boldsymbol{H}^{-1}\boldsymbol{Q} \otimes \boldsymbol{A}\right)\boldsymbol{q} + \frac{1}{\sqrt{2\rho}}\boldsymbol{H}^{-1}\boldsymbol{e}_0 \otimes \begin{bmatrix}\sigma_0 - F(v_0)\\ 0\end{bmatrix}. \tag{60}$$

Characteristic Boundary Treatment:

A similar calculation can be performed for the characteristic boundary formulation (56) and the energy dissipation rate is

$$\begin{aligned}\frac{d}{dt}\|\boldsymbol{q}(t)\|_h^2 = &-\left(\frac{w_0^- - w_0^+}{2Z}\right)\left(\frac{w_0^- + w_0^+}{2}\right)\\ &+ \left(w_0^+ - R\, w_0^-\right)\left(\sqrt{2\rho}\, v_0\Sigma_1 + \sqrt{\frac{2}{G}}\, \sigma_0\Sigma_2\right),\end{aligned} \tag{61}$$

where $R \equiv R(w_0^-)$ is the nonlinear reflection coefficient as defined in (39). By choosing $\Sigma_1 = -\Sigma_2 = 1/(2\sqrt{2\rho})$ the last term in parenthesis becomes $-w_0^+/(2Z)$ and the energy dissipation rate is

$$\begin{aligned}\frac{d}{dt}\|\boldsymbol{q}(t)\|_h^2 &= -\frac{1}{4Z}\left[\left(w_0^-\right)^2 - \left(w_0^+\right)^2\right] - \frac{1}{2Z}\left(w_0^+ - R\, w_0^-\right) w^+\\ &= -\frac{1}{4Z}\left(1 - R^2\right)\left(w_0^-\right)^2 - \frac{1}{4Z}\left(w_0^+ - R\, w_0^-\right)^2 \leq 0,\end{aligned} \tag{62}$$

which is the same rate as in the continuous problem (40) plus a numerical damping term that goes to zero as the mesh is refined. Hence the scheme is strictly stable.

The characteristic difference method is then

$$\frac{d\boldsymbol{q}}{dt} = \left(\boldsymbol{H}^{-1}\boldsymbol{Q}\otimes\boldsymbol{A}\right)\boldsymbol{q} + \frac{1}{2\sqrt{2G}}\left[w_0^+ - \mathcal{W}^+\left(w_0^-\right)\right]\boldsymbol{H}^{-1}\boldsymbol{e}_0\otimes\begin{bmatrix}-1\\1\end{bmatrix} \tag{63}$$

or, defining $\hat{\boldsymbol{q}}$ as in (51),

$$\frac{d\boldsymbol{q}}{dt} = \left(\boldsymbol{H}^{-1}\boldsymbol{Q}\otimes\boldsymbol{A}\right)\boldsymbol{q} + c_s\boldsymbol{H}^{-1}\boldsymbol{e}_0\otimes\left(\hat{\boldsymbol{q}}_0 - \boldsymbol{q}_0\right). \tag{64}$$

Remark: One interpretation of the characteristic boundary formulation for diagonal $\boldsymbol{H}$ is that the grid values $\boldsymbol{q}_0$ are being relaxed toward $\hat{\boldsymbol{q}}_0$ over the relaxation time $T = [\boldsymbol{H}]_{0,0}/c_s$. In contrast, the injection method corresponds to sudden, or instantaneous, relaxation of $\boldsymbol{q}_0$ to $\hat{\boldsymbol{q}}_0$ (compare with (50)).

3.3. Right Boundary Treatment:

In presenting both the injection and SAT methods a semi-infinite domain was assumed; of course this is not possible computationally and the domain must be truncated at some $y = y^* > 0$. As noted earlier, the material can be prestressed at a background stress σ^* and initially moving at velocity v^*. With these background values an absorbing boundary condition can be specified by setting the characteristic variable propagating into the medium at y^*, $w^-(y^*,t)$, to the constant value defined by the background values, namely

$$w^-(y^*,t) = \sigma(y^*,t) + Z\,v(y^*,t) = \sigma^* + Z\,v^* = w^*.$$

The injection method (50) is now

$$\frac{d\boldsymbol{q}}{dt} = \left(\boldsymbol{H}^{-1}\boldsymbol{Q}\otimes\boldsymbol{A}\right)\hat{\boldsymbol{q}}, \tag{65}$$

$$\hat{\boldsymbol{q}}_0 = \frac{1}{2\sqrt{2G}}\begin{bmatrix}w_0^- - \mathcal{W}^+(w_0^-)\\ w_0^- + \mathcal{W}^+(w_0^-)\end{bmatrix} \equiv \begin{bmatrix}\sqrt{\frac{\rho}{2}}\,\hat{v}_0\\ \frac{1}{\sqrt{2G}}\hat{\sigma}_0\end{bmatrix}, \tag{66}$$

$$\hat{\boldsymbol{q}}_N = \frac{1}{2\sqrt{2G}}\begin{bmatrix}w_N^+ - w^*\\ w_N^+ + w^*\end{bmatrix} \equiv \begin{bmatrix}\sqrt{\frac{\rho}{2}}\,\hat{v}_N\\ \frac{1}{\sqrt{2G}}\hat{\sigma}_N\end{bmatrix}, \tag{67}$$

$$\hat{\boldsymbol{q}}_i = \boldsymbol{q}_i, \quad i = 1,2,\ldots,N-1. \tag{68}$$

The SAT method (53) becomes

$$\frac{d\boldsymbol{q}}{dt} = \left(\boldsymbol{H}^{-1}\boldsymbol{Q} \otimes \boldsymbol{A}\right)\boldsymbol{q} + \boldsymbol{H}^{-1}\boldsymbol{e}_0 \otimes \boldsymbol{\Sigma}\boldsymbol{B}(\boldsymbol{q}_0) \tag{69}$$

$$- \frac{1}{2\sqrt{2\rho}}\left(w_N^- - w^*\right)\boldsymbol{H}^{-1}\boldsymbol{e}_N \otimes \begin{bmatrix}1\\1\end{bmatrix} \tag{70}$$

$$= \left(\boldsymbol{H}^{-1}\boldsymbol{Q} \otimes \boldsymbol{A}\right)\boldsymbol{q} \tag{71}$$

$$+ \boldsymbol{H}^{-1}\boldsymbol{e}_0 \otimes \boldsymbol{\Sigma}\boldsymbol{B}(\boldsymbol{q}_0) + c_s\boldsymbol{H}^{-1}\boldsymbol{e}_N \otimes \left(\hat{\boldsymbol{q}}_N - \boldsymbol{q}_N\right),$$

where $\boldsymbol{B}(\boldsymbol{q}_0)$ can be either boundary formulation (55) or (56) with the corresponding penalty matrix $\boldsymbol{\Sigma}$, $\hat{\boldsymbol{q}}_N$ is the same as in the injection method, and

$$\boldsymbol{e}_0 = \begin{bmatrix}1 & 0 & \cdots & 0\end{bmatrix}^T \text{ and } \boldsymbol{e}_N = \begin{bmatrix}0 & 0 & \cdots & 1\end{bmatrix}^T. \tag{72}$$

It is straightforward to show that the scheme is still strictly stable.

3.4. Non-Characteristic versus Characteristic Boundary Treatment:

Two different SAT formulations have been presented; here we look at the computational advantages and disadvantages of each. The first difference is the nature of the boundary term. For the non-characteristic method the only computational expense associated with forming the boundary term (55) is the cost of evaluating the friction law, $F(V)$. On the other hand, the characteristic boundary formulation (56) requires solving a nonlinear system in order to calculate $\mathcal{W}^+(w_0^-)$, at least when $\mathcal{W}^+(w_0^-)$ is not expressible in closed form, which involves several to many evaluations of the friction law. The net computational cost of the method is dominated by the difference approximation in the interior and in our experience the nonlinear solve is negligible in comparison.

A more important concern is related to the stiffness of the ODE, which influences the maximum time step that can be used with explicit integration methods. To understand this, consider a linear friction law,

$$F(V) = \alpha\, V \Rightarrow \mathcal{W}^+(w^-) = \frac{\alpha - Z}{\alpha + Z}w^-, \tag{73}$$

where $\alpha > 0$. The non-characteristic method is

$$\frac{d\boldsymbol{q}}{dt} = \boldsymbol{D}_{nc}\boldsymbol{q}, \tag{74}$$

$$\boldsymbol{D}_{nc} = \left(\boldsymbol{H}^{-1}\boldsymbol{Q} \otimes \boldsymbol{A}\right) \tag{75}$$

$$+ c_s\boldsymbol{H}^{-1}\boldsymbol{E}_0 \otimes \begin{bmatrix}-\alpha & 1\\ 0 & 0\end{bmatrix} - \frac{c_s}{2}\boldsymbol{H}^{-1}\boldsymbol{E}_N \otimes \begin{bmatrix}1 & 1\\ 1 & 1\end{bmatrix},$$

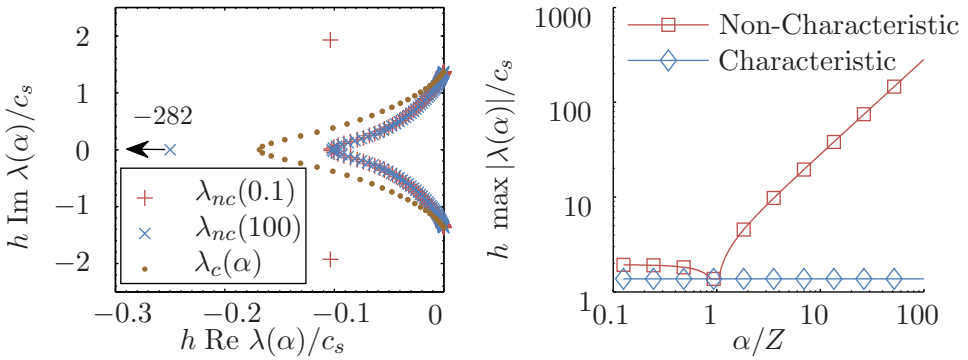

(a) Full eigenvalue spectrum

(b) Maximum magnitude eigenvalue

Figure 3: Eigenvalues for the non-characteristic and characteristic boundary treatments with the linear friction law (21). For these plots, we use $N = 50$ and the fourth order diagonal norm SBP operator; the overall trends are independent of N and the order of the operator. In (b) the spectrum $\lambda_c(\alpha)$ is largely independent of α, and for all values of α the plot is visually the same. The purely real eigenvalue of $\lambda_{nc}(100)$ is shifted to value indicated by arrow and value.

and the characteristic method is

$$\frac{d\boldsymbol{q}}{dt} = \boldsymbol{D}_c \boldsymbol{q}, \tag{76}$$

$$\boldsymbol{D}_c = \left(\boldsymbol{H}^{-1}\boldsymbol{Q} \otimes \boldsymbol{A}\right) - \frac{c_s}{Z+\alpha}\boldsymbol{H}^{-1}\boldsymbol{E}_0 \otimes \begin{bmatrix} -Z & \alpha \\ Z & -\alpha \end{bmatrix} - \frac{c_s}{2}\boldsymbol{H}^{-1}\boldsymbol{E}_N \otimes \begin{bmatrix} 1 & 1 \\ 1 & 1 \end{bmatrix}, \tag{77}$$

where the last term in $\boldsymbol{D}_{nc}$ and $\boldsymbol{D}_c$ arises from a homogeneous absorbing boundary condition ($w^* = 0$) on the right, $\boldsymbol{E}_0 = \mathbf{diag}(\boldsymbol{e}_0)$, and $\boldsymbol{E}_N = \mathbf{diag}(\boldsymbol{e}_n)$. Let $\lambda_{nc}(\alpha)$ and $\lambda_c(\alpha)$ be the eigenvalue spectra for the difference operators $\boldsymbol{D}_{nc}$ and $\boldsymbol{D}_c$, respectively, which are functions of α. In Figure 3a we show $\lambda_{nc}(0.1)$, $\lambda_{nc}(100)$, and $\lambda_c(\alpha)$ (for $\lambda_c(\alpha)$ the spectrum appears the same for all α). For both methods the whole spectrum satisfies $\mathrm{Re}\lambda \leq 0$ and for large α the non-characteristic method has a large magnitude, purely real, negative eigenvalue which leads to stiffness. We can characterize stiffness by considering the maximum magnitude eigenvalue of each spectrum, shown in Figure 3b. The figure shows that stiffness increases roughly linearly with α for the non-characteristic method (for $\alpha > 1$) and is roughly constant for the

characteristic method; the dip in the plot for the non-characteristic method is associated with a decrease in magnitude of the two "isolated" eigenvalues (seen in the spectrum of $\lambda_{nc}(0.1)$ of Figure 3a) and the increase is associated with the increase in magnitude of a single purely real, negative eigenvalue.

Linearizing a nonlinear friction law, $F(V)$, around a value V^*,

$$F(V) \approx F(V^*) + (V - V^*)\, F'(V^*), \tag{78}$$

leads to an effective value of $\alpha = F'(V^*)$; this α is different than the nonlinear $\alpha(w^-)$ defined in (38). Thus, if this effective value of α can be arbitrarily large or small, as it is for realistic friction laws commonly used in earthquake modeling, then the non-characteristic method can be arbitrarily stiff, preventing efficient solution using explicit time-stepping routines. In other words, for wave propagation problems one would like $\Delta t \sim h/c_s$, that is, a time step restriction that depends predominantly on the wave propagation properties of the problem and not the boundary treatment. This is possible for the characteristic method but not the non-characteristic method, as Figure 3 indicates. The benefits of the characteristic method significantly outweigh the drawbacks and, for this reason, the rest of this work exclusively uses characteristic boundary treatment.

Remark: If the friction law is invertible, one could imagine instead using the non-characteristic boundary condition

$$F^{-1}(\tau) = V, \tag{79}$$

which, for a semi-infinite medium, results in the method

$$\frac{d\boldsymbol{q}}{dt} = \left(\boldsymbol{H}^{-1}\boldsymbol{Q} \otimes \boldsymbol{A}\right) \boldsymbol{q} + \frac{1}{\sqrt{2\rho}} \boldsymbol{H}^{-1}\boldsymbol{e}_0 \otimes \begin{bmatrix} 0 \\ v_0 - F^{-1}(\sigma_0) \end{bmatrix}. \tag{80}$$

In this case, the maximum magnitude real eigenvalue of the difference operator scales roughly linearly with $1/\alpha$ where $\alpha = F'(V^*)$ as in (78); hence, stiffness again results but now for small α.

4. Computational Results

The formulation is tested using $c_s = 1$, $G = 1$, $y^* = 1$, and friction law

$$F(V) = 100 \operatorname{arcsinh}(100\, V). \tag{81}$$

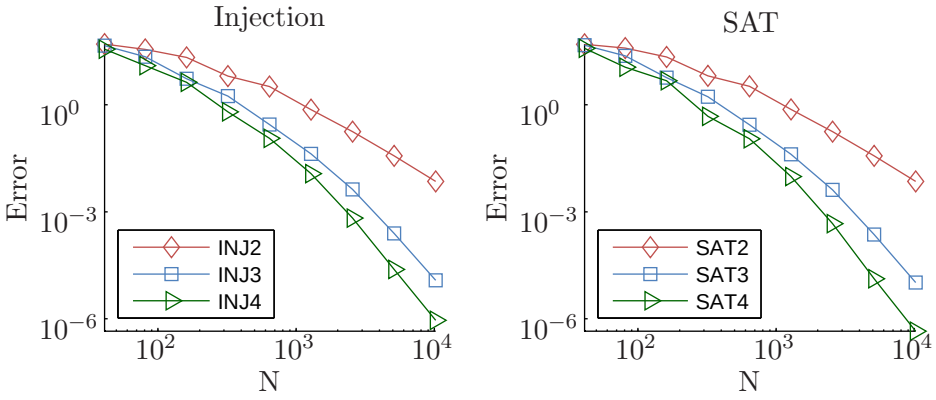

	Injection Method Rate Estimate			SAT Method Rate Estimate		
N	2^{nd}	3^{rd}	4^{th}	2^{nd}	3^{rd}	4^{th}
40	0.5	1.0	1.5	0.4	1.0	1.8
80	0.7	2.1	1.7	0.8	2.0	1.3
160	1.7	1.6	2.8	1.8	1.8	3.3
320	1.0	2.7	2.5	1.0	2.6	2.1
640	2.1	2.7	3.3	2.2	2.8	3.5
1280	2.1	3.3	4.1	2.1	3.3	4.4
2560	2.2	4.1	4.8	2.2	4.2	5.1
5120	2.4	4.4	4.7	2.4	4.5	4.9

Figure 4: Error and convergence rate estimates for the injection and SAT methods for short time integration.

The initial condition is

$$\boldsymbol{q}_i(0) = 1000\, g(y_i) \begin{bmatrix} 1 \\ 1 \end{bmatrix}, \; g(y) = \sin(20\,\pi\, y)\, \exp\left(-\frac{1}{2}\left(y - \frac{1}{2}\right)^2\right), \tag{82}$$

which corresponds to a wave packet moving to the left (into the fault). We test the 2^{nd}, 3^{rd}, and 4^{th} order accurate diagonal norm SBP operators (as determined by Strand [1994]), where the accuracy refers to their global accuracy and the interior accuracy of the methods is 2, 4, and 6, respectively. Time integration is performed with a 4^{th} order, low memory Runge-Kutta method of Carpenter and Kennedy [1994] (their 5[4] method with solution 3) using a time step $\Delta t = h/c_s$.

For the first test, time is truncated at $t_{end} = 1$ and the domain is truncated at $y^* = 1$ with a homogeneous absorbing boundary condition. Figure 4 shows the results of this test, where the error is measured using the norm defined in (46):

$$\text{error}(N) = \|\boldsymbol{q}(\cdot, t_{end}) - \boldsymbol{q}(t_{end})\|_h, \tag{83}$$

where $\boldsymbol{q}(t)$ is the $N+1$ grid point discrete solution and $\boldsymbol{q}(\cdot, t)$ is the exact solution (given in (12) and (13)) evaluated at the grid points. The convergence rate is estimated using

$$\text{p}(N) = \log\left(\frac{\text{error}(N)}{\text{error}(2\ N)}\right) \Big/ \log\left(\frac{h(N)}{h(2\ N)}\right), \tag{84}$$

where $h(N) = 1/N$. Both the injection and SAT methods perform well for this test. The fact that the injection method does well suggests that the integration time is too short for erroneous energy growth, if it exists, to affect the solution.

The energy and error growth in the solution with time can be explored by replacing the right absorbing boundary with a traction-free surface ($\sigma(1, t) = 0$ or $w^-(1, t) = -w^+(1, t)$) and integrating the solution until time $t_{end} = 201$. The wave packet interacts with the fault on the left and is reflected by the right boundary multiple ($t_{end}/2$) times. Similar boundary interactions over long times are likely to arise in practical calculations involving multiple faults, Earth's surface, and other topographic features such as sedimentary basins. This test is performed for the 3^{rd} and 4^{th} order SBP operators with $N = 400$. Figure 5 shows the error (83) and energy (46) versus time for the methods, as well as the $v(y, t)$ solution profiles at select times for the 4^{th} order methods. These plots clearly show that the energy and error grow for the injection method, whereas for the SAT method the error is bounded and energy decays at a slightly faster rate than in the exact solution, as expected.

5. Conclusions

In this paper we have considered three ways to enforce nonlinear boundary conditions in elastodynamics problems that are treated with SBP difference operators: the injection method and two forms (non-characteristic and characteristic) of the SAT method. The injection method, though conceptually straightforward, leads to a method that has a minor time instability

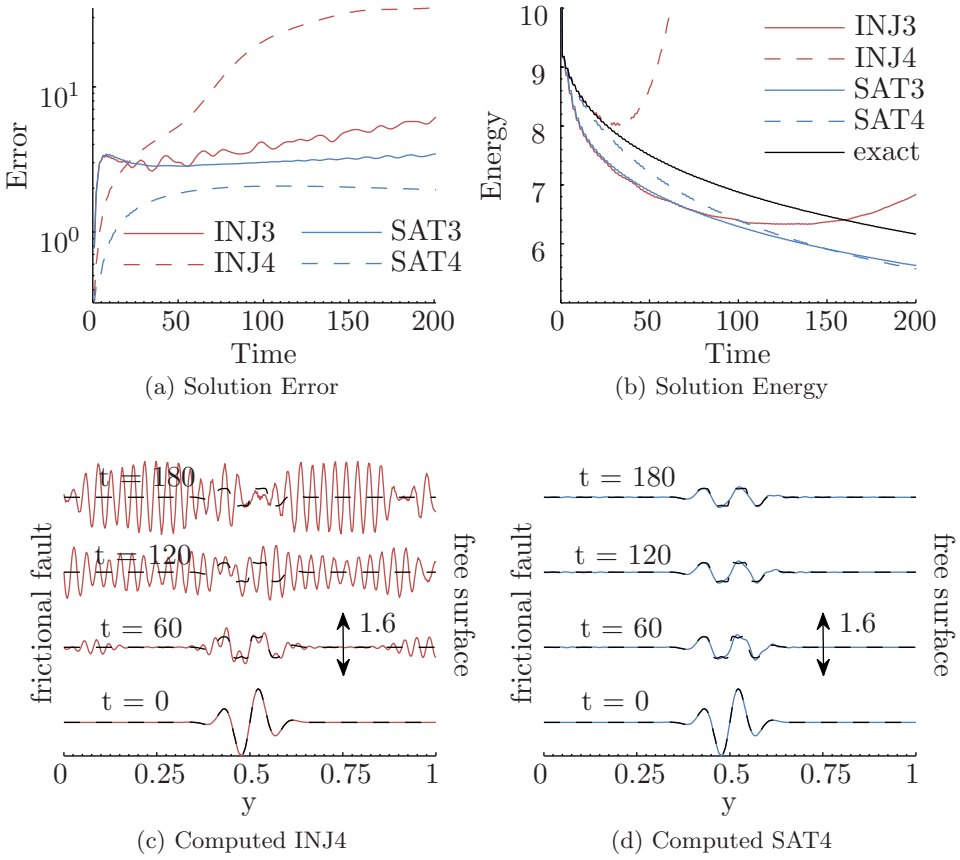

(a) Solution Error

(b) Solution Energy

(c) Computed INJ4

(d) Computed SAT4

Figure 5: Comparison of long time integration using the injection and SAT methods. Shown are the error (a), energy (b), and $v(y,t)$ for given times (c)-(d). INJ3 and INJ4 refer to the 3^{rd} and 4^{th} order injection methods and SAT3 and SAT4 the 3^{rd} and 4^{th} order SAT methods. In (c) and (d) the black dashed line is the exact solution and the red and blue lines are the computed solutions for the injection and SAT methods, respectively, at the given time.

that leads to error and energy growth for problems with long time integration. On the other hand, both SAT methods are strictly stable, leading to numerical methods that dissipate energy at least as fast as the continuous problem (additional energy dissipation goes to zero as the mesh is refined).

The characteristic SAT method uses the boundary conditions formulated in terms of the characteristic variables in the penalty term whereas the non-characteristic SAT method uses the boundary conditions formulated in terms of the physical variables. Though the non-characteristic method is slightly more straightforward to implement, it leads to an arbitrarily stiff system of ODEs whereas the characteristic method does not.

Two numerical tests confirm these results for scalar elasticity. The first test, involving short time integration, confirms that the SBP operators perform at the design order of accuracy, and results from the injection and SAT methods are comparable. The second test, involving much longer integration times, reveals that the injection method is unstable (manifesting as unphysical energy growth), whereas the SAT method is stable and dissipates energy at a slightly faster rate than the continuous problem.

In Part 2 the characteristic SAT method is generalized to full elastodynamics (involving multidirectional deformation carried by a dilatational and two shear waves with orthogonal polarizations) and faults that separate two elastic bodies with differing material properties. That work also considers the more general class of rate-and-state friction laws.

Acknowledgements

J.E.K. and E.M.D were supported by NSF-EAR award 0910574 and the Southern California Earthquake Center (SCEC), as funded by Cooperative Agreements NSF-EAR 0106924 and USGS 02HQAG0008 (SCEC contribution number 1417).

A. Well-posedness for $F'(V) \neq -Z$

In the text of the paper it was required, for well-posedness, that $F(V)V \geq 0$ and $F'(V) \geq 0$. Though all physically realistic friction laws satisfy this requirement, it is possible to show that the problem is well-posed under the less-restrictive condition $F'(V) \neq -Z$. In what follows we assume that $F(V)$ is smooth for all V. Additionally, the problem with a frictional boundary on the right at $y = L$ (as opposed to the semi-infinite problem) is considered as it is the more complex case; the semi-infinite problem is a straightforward extension of what follows. We allow for two frictions laws, $\tau = F_0(V_0)$ on

the left and $\tau = F_L(V_L)$ on the right, and will show that the problem is well-posed as long as $F_0'(V_0)$ and $F_L'(V_L)$ are bounded away from $-Z$. Note that for the right boundary the slip velocity is defined as $V_L(t) = -v(L,t)$ and the fault strength as $\tau(t) = \sigma(L,t)$.

Consider the problem in characteristic form (9) with boundary conditions

$$w^+(0,t) = \mathcal{W}^+\left(w^-(0,t)\right) = R_0\left(w^-(0,t)\right) w^-(0,t), \tag{85}$$
$$w^-(L,t) = \mathcal{W}^-\left(w^+(L,t)\right) = R_L\left(w^+(L,t)\right) w^+(L,t), \tag{86}$$

and initial data $\boldsymbol{w}(y,0) = \boldsymbol{w}_0$. Defining the norm

$$\|\boldsymbol{w}\|_\delta^2 = \int_0^L \boldsymbol{w}^T \begin{bmatrix} e^{-\delta(L-y)} & 0 \\ 0 & e^{-\delta y} \end{bmatrix} \boldsymbol{w}\, dy, \tag{87}$$

we have the energy dissipation rate

$$\begin{aligned}
\frac{d}{dt}\|\boldsymbol{w}\|_\delta^2 =& 2c_s \int_0^L \boldsymbol{w}^T \begin{bmatrix} -e^{-\delta(L-y)} & 0 \\ 0 & e^{-\delta y} \end{bmatrix} \frac{\partial \boldsymbol{w}}{\partial y}\, dy \\
=& -c_s\left[\left(w^+\right)^2 - e^{-\delta L}\left(w^-\right)^2\right]_{y=L} - c_s\left[\left(w^-\right)^2 - e^{-\delta L}\left(w^+\right)^2\right]_{y=0} \\
&+ c_s\delta \int_0^\infty \boldsymbol{w}^T \begin{bmatrix} e^{-\delta(L-y)} & 0 \\ 0 & e^{-\delta y} \end{bmatrix} \boldsymbol{w}\, dy \\
=& -c_s\left[1 - e^{-\delta L} R_L\left(w^+\right)^2\right]\left(w^+\right)^2\Big|_{y=L} \\
&- c_s\left[1 - e^{-\delta L} R_0\left(w^-\right)^2\right]\left(w^-\right)^2\Big|_{y=0} + c_s\delta\|\boldsymbol{w}\|_\delta^2.
\end{aligned} \tag{88}$$

If $|R_0(w^-)|$, $|R_L(w^+)| \le C < \infty$ for some positive constant C then we can choose $\delta \ge 0$ such that $e^{-\delta L} \le 1/C$, or $\delta \ge \ln(C)/L$, and (88) becomes

$$\frac{d}{dt}\|\boldsymbol{w}\|_\delta^2 \le c_s\delta\|\boldsymbol{w}\|_\delta^2. \tag{89}$$

Thus, we have an energy estimate of the form (14) with $\alpha_c = c_s\delta$.

From (31) we know that if $F_0'(V_0) \neq -Z$ then we can assume the boundary condition is $w^-(0,t) = \mathcal{W}^+(w^-(0,t))$. If we can show that $F_0'(V_0)$ bounded away from $-Z$ implies $R_0(w) \le C < \infty$, then the energy estimate holds for the physical variables as well. We will only show this for the left boundary and a completely analogous argument applies to the right boundary. Using the friction law $\tau = F_0(V_0)$ and the characteristic variables

(9), the reflection coefficient can be written in terms of V_0:

$$w^+ = \frac{w^+}{w^-} w^- = \frac{\tau - ZV_0}{\tau + ZV_0} w^- = \frac{F_0(V_0) - ZV_0}{F_0(V_0) + ZV_0} w^- = R_0(V_0) w^-, \quad (90)$$

$$R_0(V_0) = \frac{F_0(V_0) - ZV_0}{F_0(V_0) + ZV_0}. \quad (91)$$

In order to show that $R_0(V_0)$ is bounded we consider where the extrema occur, namely, $R_0'(V_0) = 0$ if $V_0 = F_0(V_0)/F_0'(V_0)$. Using this in (91) gives

$$R_0\left(\frac{F_0(V_0)}{F_0'(V_0)}\right) = \frac{F_0'(V_0) - Z}{F_0'(V_0) + Z}, \quad (92)$$

which is bounded if $F_0'(V_0)$ is bounded away from $-Z$. Hence we have that $|R_0(V_0)| \leq C < \infty$ if $F_0'(V_0) \geq -Z + \varepsilon$ or $F_0'(V_0) \leq -Z - \varepsilon$ for some $\varepsilon > 0$.

We must also check what happens in the $\lim_{|V_0| \to \infty} R_0(V_0)$. This is only a problem if the numerator of $R_0(V_0)$ goes to $\pm\infty$, since the denominator is always nonzero. If the numerator goes to $\pm\infty$ then the denominator also goes to $\pm\infty$ and L'Hôpital's rule can be used to show that $R_0(V_0)$ is bounded. Hence, we have shown that if $F_0'(V_0)$ is bounded away from $-Z$ then $R_0(V_0)$ is bounded and the energy estimate holds.

All that remains for the problem to be well-posed is that the solution must be unique; existence of a solution follows from the method of characteristics and the fact that if $F_0(V)$ and $F_L(V)$ are bounded away from $-Z$ then they lead to unique characteristic boundary conditions. Assume that we have two solutions $\boldsymbol{q}_1$ and $\boldsymbol{q}_2$ with the same initial data. The difference of the solutions $\Delta\boldsymbol{q} = \boldsymbol{q}_1 - \boldsymbol{q}_2$ satisfies (8) with zero initial data and boundary conditions

$$\Delta\sigma(0,t) = F_0(v_1(0,t)) - F_0(v_2(0,t)), \quad (93)$$

$$\Delta\sigma(L,t) = F_L(v_1(L,t)) - F_L(v_2(L,t)). \quad (94)$$

Using the mean value theorem we have that these boundary conditions can be rewritten as

$$\Delta\sigma(0,t) = F_0'(V_0(t))\, \Delta v(0,t), \quad (95)$$

$$\Delta\sigma(L,t) = F_L'(V_L(t))\, \Delta v(L,t), \quad (96)$$

for some $V_0(t) \in [v_1(0,t), v_2(0,t)]$ and $V_L(t) \in [v_1(L,t), v_2(L,t)]$. Transforming to the characteristic form of the problem (9) the boundary conditions

become

$$\Delta w^+(0,t) = \frac{F_0'(V_0(t)) - Z}{F_0'(V_0(t)) + Z}\,\Delta w^-(0,t) = \Delta R_0(V_0(t))\,\Delta w^-(0,t), \tag{97}$$

$$\Delta w^-(L,t) = \frac{F_L'(V_L(t)) - Z}{F_L'(V_L(t)) + Z}\,\Delta w^+(L,t) = \Delta R_L(V_L(t))\,\Delta w^-(L,t), \tag{98}$$

and if $F_0'(V_0)$ and $F_L'(V_L)$ are bounded away from $-Z$ then $|\Delta R_0(V_0)|$ and $|\Delta R_L(V_L)|$ are bounded away from ∞. The solution difference thus satisfies the energy estimate

$$\|\Delta \boldsymbol{w}(\cdot,t)\|_\delta^2 \leq e^{c_s\delta}\|\Delta \boldsymbol{w}(\cdot,0)\|_\delta^2 = 0, \tag{99}$$

for some $\delta \geq \ln(C)$, see (89), and uniqueness follows.

Remark: For the semi-infinite problem one can use the norm

$$\|\boldsymbol{w}\|_\delta^2 = \int_0^L \boldsymbol{w}^T \begin{bmatrix} \delta & 0 \\ 0 & 1 \end{bmatrix} \boldsymbol{w}\; dy, \tag{100}$$

and pick a $\delta > 0$ such that $\|\boldsymbol{w}\|_\delta^2 \leq 0$ and thus there is no exponential energy growth. If $\delta < 1$ the energy estimate in terms of the physical variables has $K_c > 1$ in (14), and thus there can be an energy increase but only by a constant scaling factor.

Remark: If the friction laws satisfy $F_0(V_0)V_0 \geq 0$ and $F_L(V_L)V_L \geq 0$ then by (26) $\|\boldsymbol{q}(\cdot,t)\|^2 \leq \|\boldsymbol{q}(\cdot,0)\|^2$ and the problem dissipates energy in the physical variables even if $F_0'(V) < 0$ or $F_L'(V) < 0$ for some values of V (this is the case shown in Figure 2b).

References

M. H. Carpenter, D. Gottlieb, and S. Abarbanel. Time-stable boundary conditions for finite-difference schemes solving hyperbolic systems: Methodology and application to high-order compact schemes. *J. Comp. Phys.*, 111(2):220–236, 1994. doi: 10.1006/jcph.1994.1057.

M. H. Carpenter, J. Nordström, and D. Gottlieb. A stable and conservative interface treatment of arbitrary spatial accuracy. *J. Comp. Phys.*, 148(2): 341–365, 1999.

M.H. Carpenter and C.A. Kennedy. Fourth-order 2N-storage Runge-Kutta schemes. Technical Report NASA TM-109112, National Aeronautics and Space Administration, Langley Research Center, Hampton, VA, 1994.

A. Cochard and R. Madariaga. Dynamic faulting under rate-dependent friction. *Pure Appl. Geophys.*, 142(3):419–445, 1994. doi: 10.1007/BF00876049.

P. H. Geubelle and J. R. Rice. A spectral method for three-dimensional elastodynamic fracture problems. *J. Mech. Phys. Solids*, 43(11):1791–1824, 1995. doi: 10.1016/0022-5096(95)00043-I.

B. Gustafsson. The convergence rate for difference approximations to mixed initial boundary value problems. *Math. Comp.*, 29(130):396–406, 1975.

B. Gustafsson, H.-O. Kreiss, and J. Oliger. *Time Dependent Problems and Difference Methods*. Wiley-Interscience, 1996.

H.-O. Kreiss. Initial boundary value problems for hyperbolic systems. *Com. Pure Appl. Math.*, 23(3):277–298, 1970. doi: 10.1002/cpa.3160230304.

H.-O. Kreiss and G. Scherer. Finite element and finite difference methods for hyperbolic partial differential equations. In *Mathematical aspects of finite elements in partial differential equations; Proceedings of the Symposium*, pages 195–212, Madison, WI, 1974.

H.-O. Kreiss and G. Scherer. On the existence of energy estimates for difference approximations for hyperbolic systems. Technical report, Dept. of Scientific Computing, Uppsala University, 1977.

L. E. Malvern. *Introduction to the Mechanics of a Continuous Medium*. Prentice Hall, 1st edition, 1977.

K. Mattsson. Boundary procedures for summation-by-parts operators. *J. Sci. Comp.*, 18(1):133–153, 2003. doi: 10.1023/A:1020342429644.

K. Mattsson and J. Nordström. Summation by parts operators for finite difference approximations of second derivatives. *J. Comp. Phys.*, 199(2): 503–540, 2004. doi: 10.1016/j.jcp.2004.03.001.

J. Nordström. Conservative finite difference formulations, variable coefficients, energy estimates and artificial dissipation. *J. Sci. Comp.*, 29(3): 375–404, 2006. doi: 10.1007/s10915-005-9013-4.

J. Nordström and M. H. Carpenter. High-order finite difference methods, multidimensional linear problems, and curvilinear coordinates. *J. Comp. Phys.*, 173(1):149–174, 2001. doi: 10.1006/jcph.2001.6864.

J. Oliger and A. Sundstrom. Theoretical and practical aspects of some initial boundary value problems in fluid dynamics. *SIAM J. Appl. Math.*, 35(3): 419–446, 1978.

P. Olsson. Summation by parts, projections, and stability. II. *Math. Comp.*, 64(212):1473–1493, 1995.

J. R. Rice. Spatio-temporal complexity of slip on a fault. *J. Geophys. Res.*, 98(B6):9885–9907, 1993. doi: 10.1029/93JB00191.

B. Strand. Summation by parts for finite difference approximations for d/dx. *J. Comp. Phys.*, 110(1):47–67, 1994. doi: 10.1006/jcph.1994.1005.

M. Svärd and J. Nordström. On the order of accuracy for difference approximations of initial-boundary value problems. *J. Comp. Phys.*, 218(1): 333–352, 2007.

K. W. Thompson. Time dependent boundary conditions for hyperbolic systems. *J. Comp. Phys.*, 68(1):1–24, 1987. doi: 10.1016/0021-9991(87)90041-6.

K. W. Thompson. Time-dependent boundary conditions for hyperbolic systems, II. *J. Comp. Phys.*, 89(2):439–461, 1990. doi: 10.1016/0021-9991(90)90152-Q.